Latest Pleistocene and Holocene river network evolution in the Ethiopian Lakes Region

Mario Sagri [a], Carlo Bartolini [a,*], Paolo Billi [b], Giovanni Ferrari [c], Marco Benvenuti [a], Stefano Carnicelli [c], Francesco Barbano [c]

[a] *Dipartimento di Scienze della Terra, Università di Firenze, Via La Pira, 4, 50121 Firenze, Italy*
[b] *Dipartimento di Scienze della Terra, Università di Ferrara, Via G. Saragat, 1, 44100 Ferrara, Italy*
[c] *Dipartimento di Scienza del Suolo e Nutrizione della Pianta, Università di Firenze, P.le Cascine, 15, 50144 Firenze, Italy*

Abstract

River network, geomorphologic, paleohydrologic, stratigraphic and sedimentologic analyses document a dramatic reorganization of the drainage pattern in the northern part of the Main Ethiopian Rift (MER) during latest Pleistocene and early Holocene. The river network modification was induced by tectonic deformation, volcanic activity, and by the arid conditions connected with the Last Glacial Maximum (LGM). This arid phase triggered the shrinking of a Pleistocene Megalake that formerly flooded large part of the Main Ethiopian Rift. The northern tributaries (paleo-Awash and paleo-Mojo rivers) extended, following the lake shore retreat, and incised the Fesesa, Koye, and Cheleleka-Sulula Hafa paleovalleys through the Pleistocene deposits. At the beginning of the Holocene, humid conditions induced a water-level rise in the lacustrine basin (Ziway–Shala basin), supplied from the north by the large Awash–Mojo–Meki fluvial system. A well exposed cross-section of the Cheleleka paleovalley at the confluence with the Meki River and the use of paleohydrological methods allowed to infer the bankfull paleo-discharge of the larger Awash-Mojo river system. Tectonic events allowed the Awash and Mojo rivers to divert their courses to the east toward the Afar depression, depriving the Ziway–Shala lacustrine basin of large volumes of water supply. This and the further increase in aridity during the late Holocene led to the separation of the Ziway–Shala paleolake into the present four lakes (Ziway, Langano, Abjiata, Shala). This study indicates that in the Main Ethiopian Rift, climatic changes cannot be inferred from lake-level variations alone because changes in water supply are also influenced by the tectonic-induced rearrangement of the fluvial drainage networks.
© 2007 Elsevier B.V. All rights reserved.

Keywords: Drainage evolution; Paleohydrology; Lake-level variations; Climatic changes; Ethiopian Rift; Late Quaternary

1. Introduction

The endoreic lacustrine systems in the Main Ethiopian Rift (MER) and the Afar depression (Figs. 1 and 2A), have long been considered as ideal settings for the study of Late Quaternary climatic fluctuations (Gillespie et al., 1983; Coetzee and van Zinderen Bakker, 1989; Gasse and Van Campo, 1994). Evidence of climatic and environmental changes was inferred by several authors through geomorphic, stratigraphic, sedimentologic (Gèze, 1975; Gasse and Street, 1978; Street, 1979; Gasse and Fontes, 1988; Alessio et al., 1996; Le Turdu et al., 1999; Benvenuti et al., 2002; Carnicelli et al., 2002) and paleolimnic analyses (Bonnefille et al., 1986; Lamb et al., 2000; Charlié and Gasse, 2002).

* Corresponding author.
E-mail address: c.bartolini@steno.geo.unifi.it (C. Bartolini).
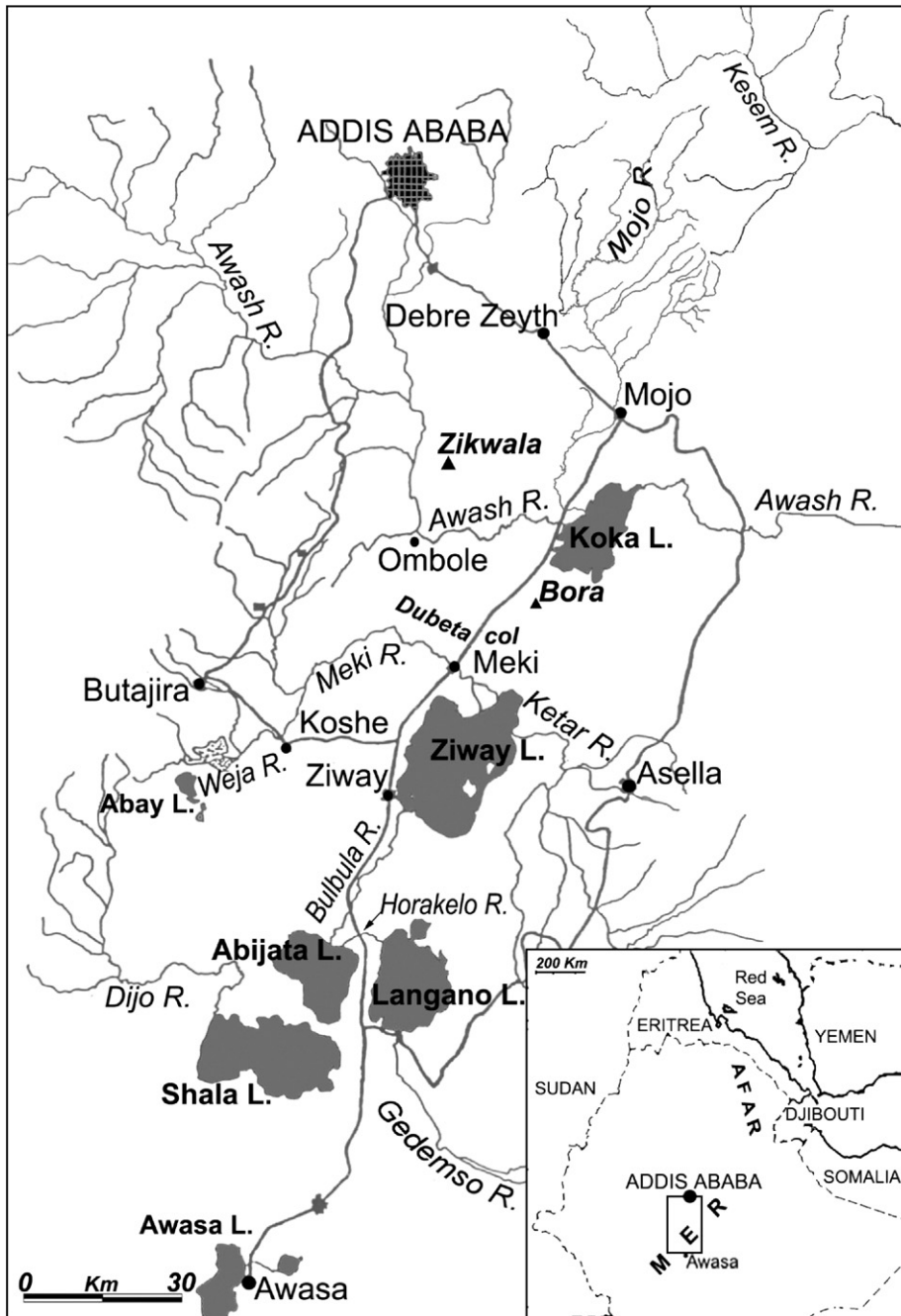
Fig. 1. Location map of the study area.

Street and Grove (1979) estimated such Late Quaternary climatic parameters as temperature and rainfall in the Main Ethiopian Rift , whereas investigations on Lake Abbe, located in the Afar depression, led Gasse (1977) to infer rainfall variations in the Ethiopian highlands during Late Pleistocene and Holocene.

Lake level oscillations in the MER were interpreted as mainly driven by climatic changes (e.g. Gasse and Street, 1978; Street, 1979). The potential influence of tectonics and volcanism were usually not taken into account, though these forces were active during Late Quaternary, and potentially capable of inducing changes in the drainage networks, and then in the water balance of lacustrine basins (Benvenuti et al., 2002).

The objective of this paper is to analyse and discuss geomorphologic, palaeohydrologic, sedimentologic,
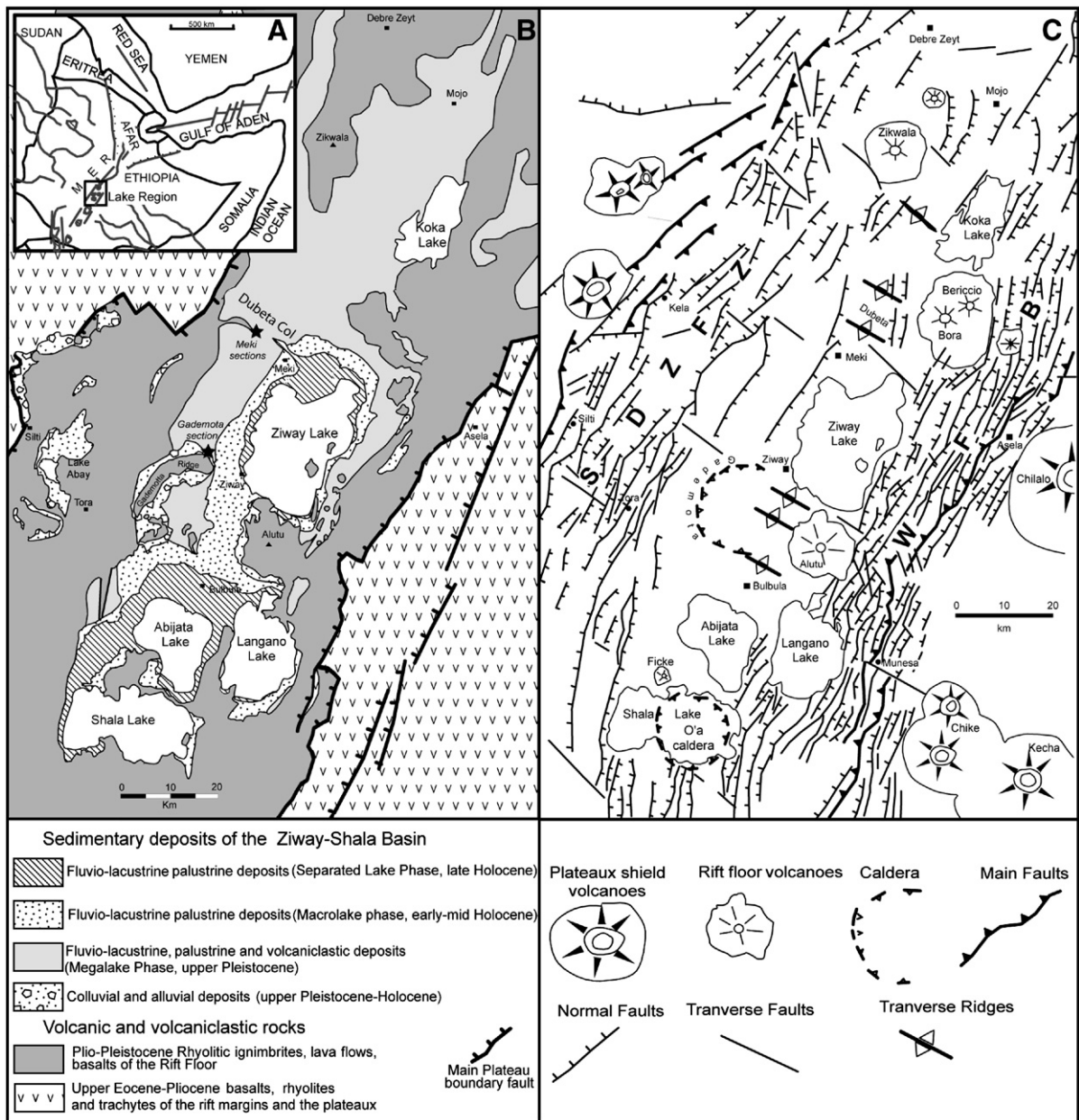
Fig. 2. Maps of the study area. (A) Location of the Lakes Region within the Main Ethiopian Rift (MER) (rectangle indicates study area); (B) simplified geological map; (C) structural sketch map and major volcanic edifices, Wongj Fault Belt (WFB), Silti–Debre Zeyt Fault Zone (SDZFZ).

structural and geologic evidences of major Late Quaternary drainage network rearrangements in the northern portion of the MER.

2. General setting

2.1. Morphology

The Lakes Region is located in the northern portion of the MER (Fig. 2A), a NNE-elongated depression,

80 km wide by 700 km long and bounded by stepped escarpments, leading to the Ethiopian and Somali plateaux. It includes Koka reservoir, fed by the Awash and Mojo rivers, to the north and, to the south, the endoreic Ziway–Shala lake basin, including the Ziway, Shala, Langano, and Abijata lakes (Fig. 1). The Ziway and Langano lakes drain into the Abijata via, respectively, the Bulbula and Horakelo rivers, whereas Lake Shala forms a separate basin, partly fed by groundwater seepage from the other lakes (Street, 1979; Chernet,

1982). The main feeding rivers, the Meki and Ketar, enter Lake Ziway and form large progradational deltas.

The average elevation of the Ziway–Shala basin is about 1600 m asl. It gently decreases from about 1640 m at Ziway lake to about 1580 m at the Abijata and Shala shorelines. Low-lying, transverse thresholds subdivide the Rift floor; one such threshold (Dubeta col) forms the divide between the Awash river and the Meki river (Figs. 1 and 2B).

Volcanic edifices (such as Alutu, Bora-Bericcio, Zikwala; Fig. 2C) rise up to 1500 m above the plain. The two border areas of the MER are strongly affected by the Wonji Fault Belt (WFB) and the Silti–Debre Zeyt Fault Zone (SDZFZ) (Mohr, 1962; Di Paola, 1972) (Fig. 2C) and show an uneven topography with narrow valleys and uplifted blocks, lava fields, spatter cones, and swampy depressions.

On both sides of the Rift, the plateaux rise to an average altitude of 2500 m asl and large shield volcanoes, up to 4000 m high, stand on them. Late Quaternary glacial cirques and moraines are found on top of a few of these mountains (Grove et al., 1975).

2.2. Geology

The MER and its flanks are made of Tertiary to Quaternary volcanites and pyroclastic rocks, whereas large areas of the Rift floor are covered by upper Quaternary volcano–lacustrine, fluvio–lacustrine, and colluvial deposits (Fig. 2B).

Modern lakes Ziway, Shala, Langano and Abijata, are relics of a large lake that, at times, occupied most of the MER floor (Merla et al., 1979; Tefera et al., 1996; Benvenuti et al., 2002). At least two major stages of lake expansion are documented (Street, 1979; Gillespie et al., 1983; Alessio et al., 1996; Le Turdu et al., 1999; Benvenuti et al., 2002). They were summarised as the Late Pleistocene Megalake and the early–middle Holocene Macrolake phases by Benvenuti et al. (2002). Conversely, two main phases of lake shrinking occurred during the latest Pleistocene and late Holocene, representing the Reduced Lakes phase and the Separated Lakes phase of Benvenuti et al. (2002). At its maximum extension, the Macrolake was notably smaller than the Megalake (Fig. 2B). The latter extended as far north as Mojo and Debre Zeyt, whereas the maximum Macrolake extension has always been considered as controlled by an overflow threshold, Dubeta col, at 1670 m asl (Street, 1979; Benvenuti et al., 2002).

The Rift shoulders are displaced by a series of NNE-trending normal faults, accommodating total offsets of 1500 to 2000 m between the Rift floor and the surrounding plateaux (Di Paola, 1972; Abbate and Sagri, 1980; Woldegabriel et al., 1990; Chorowicz et al., 1994; Abebe et al., 2005). The Rift floor is affected by Late Quaternary, closely-spaced faulting along the Wonji and Silti–Debre Zeyt fault belts, to the east and to the west, respectively (Fig. 2C). In some places, NW-trending transverse faults truncate the Rift-wise faults of the plateau margins (Di Paola, 1972; Woldegabriel et al., 1990; Le Turdu et al., 1999; Fig. 2C).

The fault pattern of the MER has been interpreted as due either to a continuous NW-SE extension or to a more complex polyphase deformation. Pure extension has been related to a single phase acting from Miocene to present (Di Paola, 1972; Woldegabriel et al., 1990; Ebinger et al., 1993; Acocella and Korme, 2002). The polyphase model, instead, includes a Miocene–Pliocene orthogonal extension followed by a Quaternary oblique-slip rifting (Bonini et al., 1997; Boccaletti et al., 1998). The first phase of orthogonal extension formed the major boundary faults, whereas the more recent oblique rifting, with E–W extension, formed the Late Quaternary Wonji and Silti–Debre Zeyt fault belts. The more recent phase of deformation gave rise to open anticlines, deforming the Late Quaternary deposits of the rift floor (Benvenuti et al., 2002) and to the eastward tilting of the Rift floor.

2.3. Modern climate and palaeoclimatic variations

The study area belongs to the tropical wet and dry class of the Köppen classification, and is a semi-arid dryland according to the Thornthwaite climate index-based classification (Meigs, 1953; Graf, 1988). Modern MER climate is influenced by the annual shift of the Intertropical Convergence Zone (ITCZ) and by physiography. Northward migration of the ITCZ during the boreal spring produces the Little Rain season (Belgh in Amharic), whereas the Big Rains (Kiremt) coincide with the northernmost position of the ITCZ during the boreal summer, and with an inland convergence of moist airstreams from the Congo Basin and the Indian Ocean. The southernmost shift of the ITCZ, during boreal winter, leads to the dry period, when a subtropical high stands to the north of Ethiopia and dry north-easterly winds blow from the Arabian Peninsula.

The central portion of the MER is the driest, as annual rainfall may drop to less than 600 mm and mean annual temperature is over 20 °C, with a potential evaporation higher than 2000 mm year^{-1} (pan evaporation data) and a potential evapotranspiration (Thornthwaite method) of about 900 mm year^{-1} (Billi, 1998). On the MER margins, the climate is moister, with

around 1200 mm yearly rainfall, and cooler, giving rise to a denser vegetation and the common occurrence of grasslands also during the dry spell.

Mean monthly minimum temperature increases slightly from the MER margins to the bottom with lowest values in January (10–12 °C, respectively) and a maximum of less than 15 °C in June–July. The highest

mean monthly temperatures occur in February–March (22–29 °C) and decrease to their minimum value in July–August (20–25 °C), that is during the Kiremt.

During the last 100,000 years the MER experienced dramatic paleohydrological variations; large lake systems developed during both Last Glacial interstadials and the early-mid Holocene climatic optimum. Major
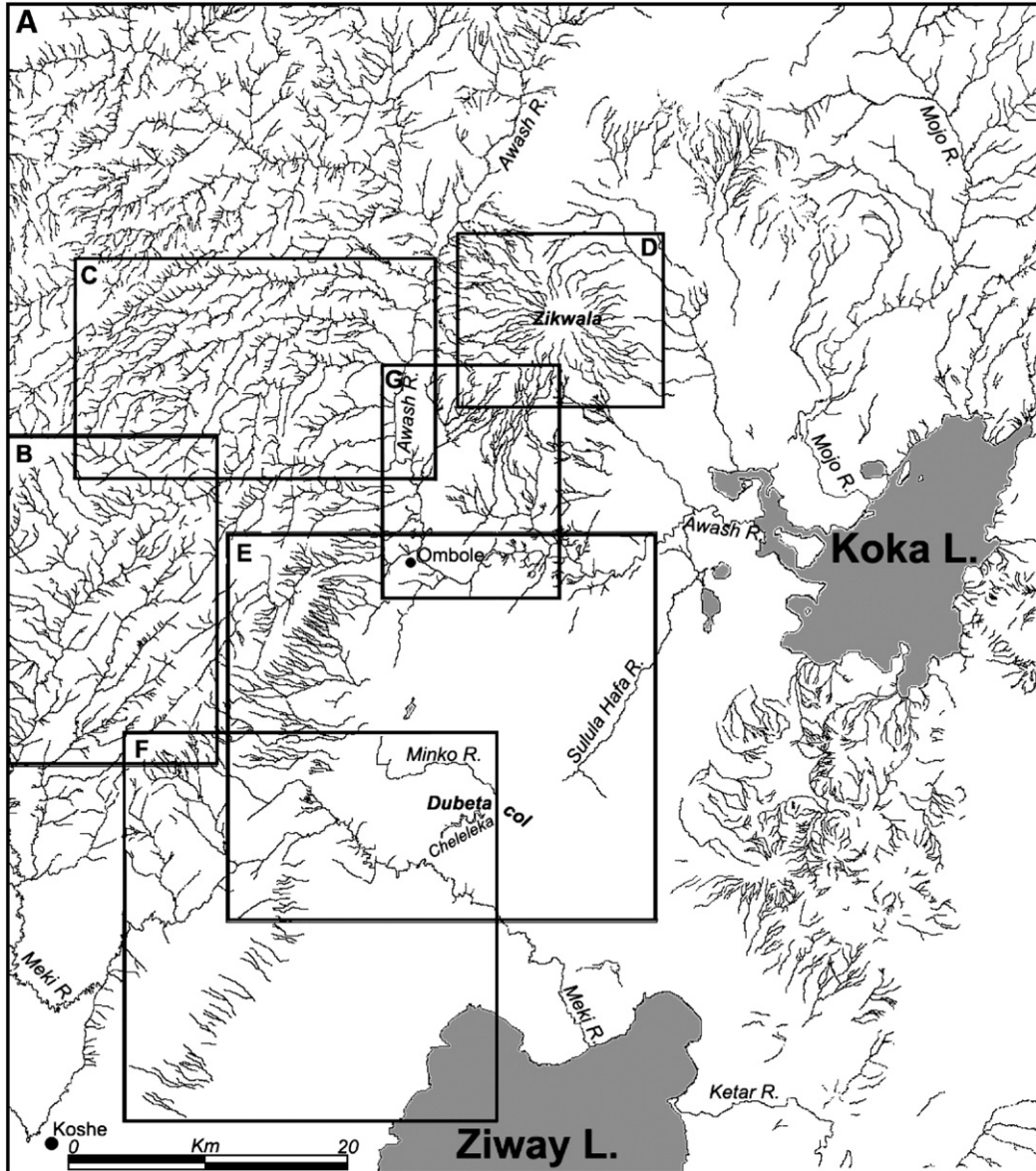

Fig. 3. (A) Drainage pattern of the study area (redrawn from 1:50,000 topographic map of Ethiopia, Alem Tena, Bui, Gonde, Koka, Koshe, Meki, Melka Kunture, Mojo and Zikwala Sheets). Insets refer to Fig. 3B–G; (B) drainage network controlled by north-easterly trending fractures and faults as well as by the south-easterly trending regional slope; (C) right hand tributaries of the Awash river, flowing from the Western Plateau rim and showing a featherlike drainage largely controlled by the regional slope; (D) typical radial drainage on Zikwala Volcano; (E) areas with very different river density on the rift margin and on the rift floor; (F) ephemeral streams disconnected from the main river system; (G) the Awash river near Ombole village lacking its left-hand tributaries, which have been captured, through headward erosion, by the Fincha river, actively fed by the Zikwala high density drainage.
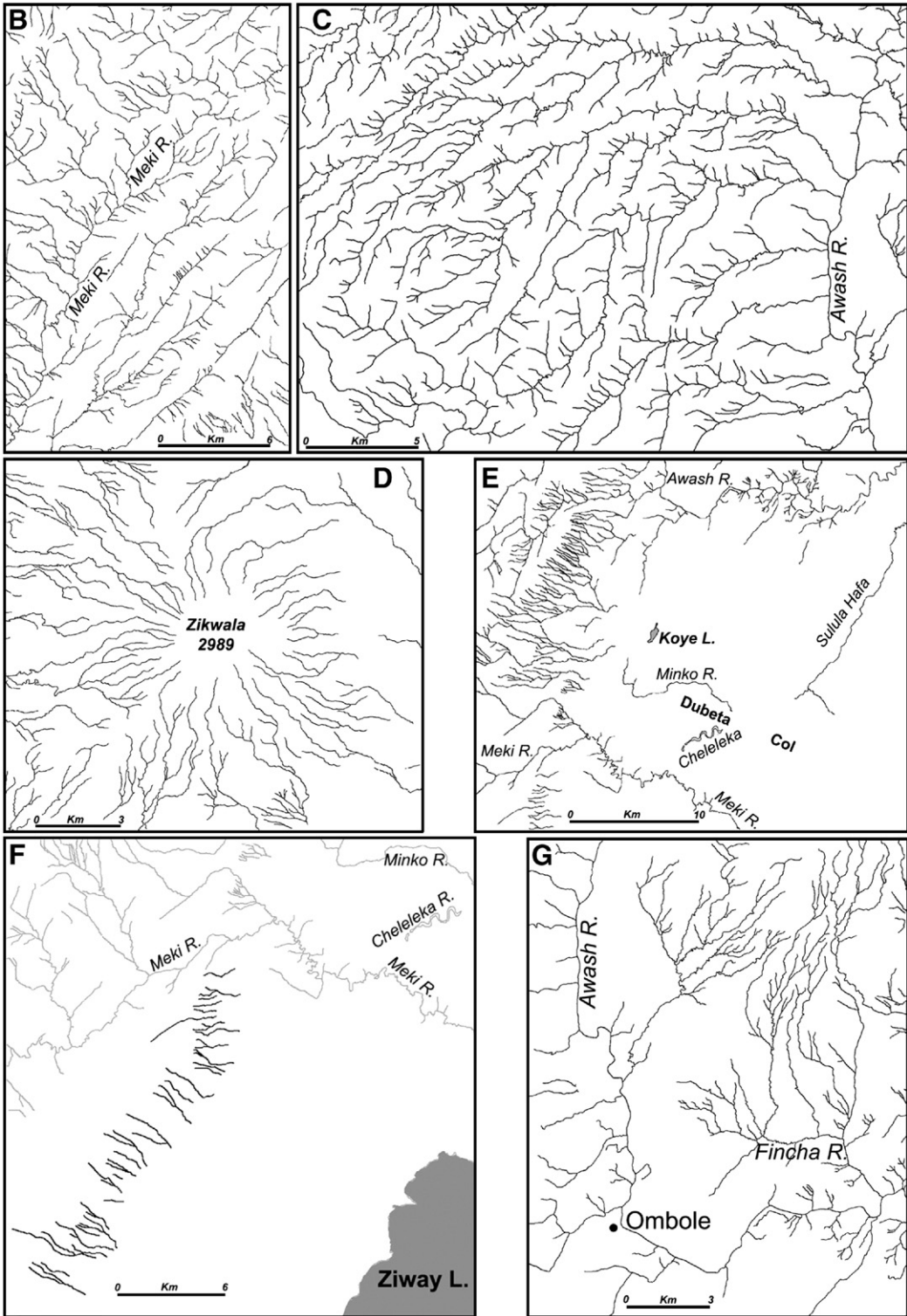
Fig. 3 (*continued*).

lakes' lowerings occurred during the latest Pleistocene, approximately around the Last Glacial Maximum, and in the last 5000 years. In reconstructing this history, the authors (Gasse and Street, 1978; Street, 1979; Gillespie et al., 1983), proposed a new interpretation for the Late Quaternary dynamics of tropical lakes. This model, expressed by a strict link between high stands and high global temperatures, defined a general "warm-moist vs. cold-dry" paradigm of intertropical climate variations, superseded the previously prevailing "pluvial" paradigm, postulating the opposite relation between temperature and rainfall (Coetzee and van Zinderen Bakker, 1989).

3. Late Quaternary evolution of the drainage network

In order to understand whether lake level oscillations can be associated with or were affected by the drainage evolution of the northern portion of the MER, geomorphologic, stratigraphic, sedimentologic and palaeohydrologic data were obtained from satellite images, aerial photographs, topographic maps and field surveys to trace the former river network and its changes during Late Pleistocene and Holocene.

3.1. River network

In the MER, the drainage networks are variable in terms of typology, orientation, and density , as they are affected by different factors from place to place (Fig. 3A). Within the Rift, the river pattern seems dependent on the rift-wise fractures and faults as well as the main regional slope (Fig. 3B) due to the eastward tilting of the Rift floor. Such trends clearly appear in the rose diagrams when first and fifth order river segments directions are compared (Fig. 4). Moreover, since in general first order segments are newly formed water courses while fifth order segments exist since a longer time, the constrain due to regional slope forcing appears to be a relatively recent feature.

The influence of the regional slope is dominant and it is observed in several areas of the Rift margins (such as the right-hand tributaries of the Awash River), where a featherlike drainage pattern is visible (Fig. 3C). By contrast, a radial drainage is on volcanoes where annular patterns have not yet developed, given their recent age (Fig. 3D).

In the study area, drainage density is widely affected by both highly variable bedrock lithology and regional slope (Fig. 3 E). The combination of a semi-arid climate, with strong decadal to millennial variations, and of a highly dynamic relief causes the frequent occurrence of discontinuous ephemeral streams (DES, Bull, 1997; Fig. 3F).
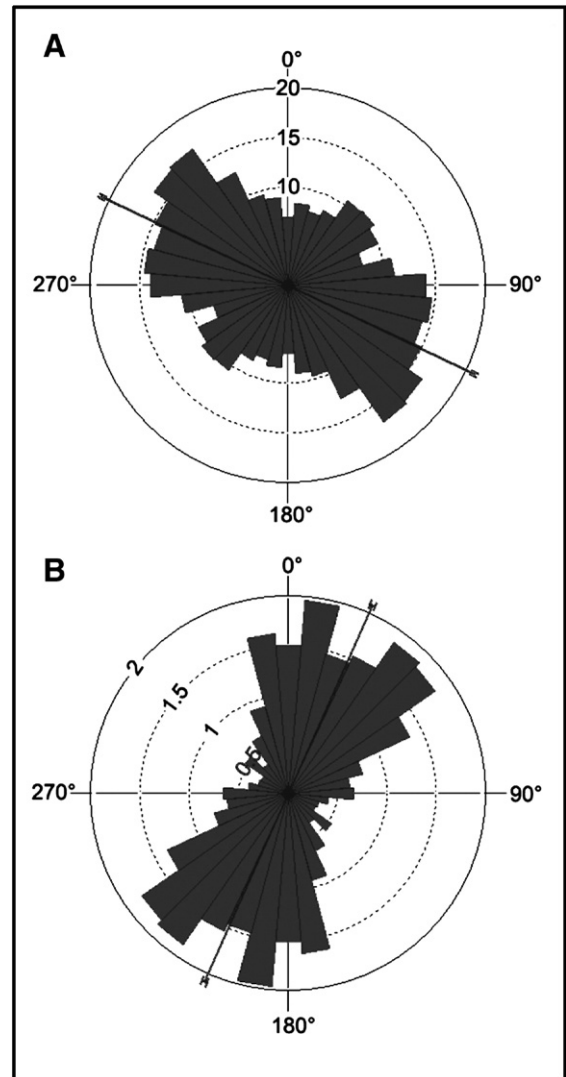

Fig. 4. Rose diagrams of the first order (A) and fifth order segments (B) of the drainage shown in Fig. 3B.

The large number and the spatially uniform distribution within the study area of stream piracies can be accounted for by recent development of an eastward regional slope, following tilting of the Rift floor. Near Ombole the Awash river is devoid of left-hand tributaries, which were captured by the Fincha river (actively fed by the Zikwala high density drainage) through headward erosion (Fig. 3G). Furthermore, the drainage rearrangement of the main river trunks turning from southwesterly to easterly directions reflects the generalised tilting of the Rift floor. The combined influence of structural control, regional slope, and stream piracy has resulted in peculiar drainage patterns such as those depicted in Fig. 5A and B. For instance,
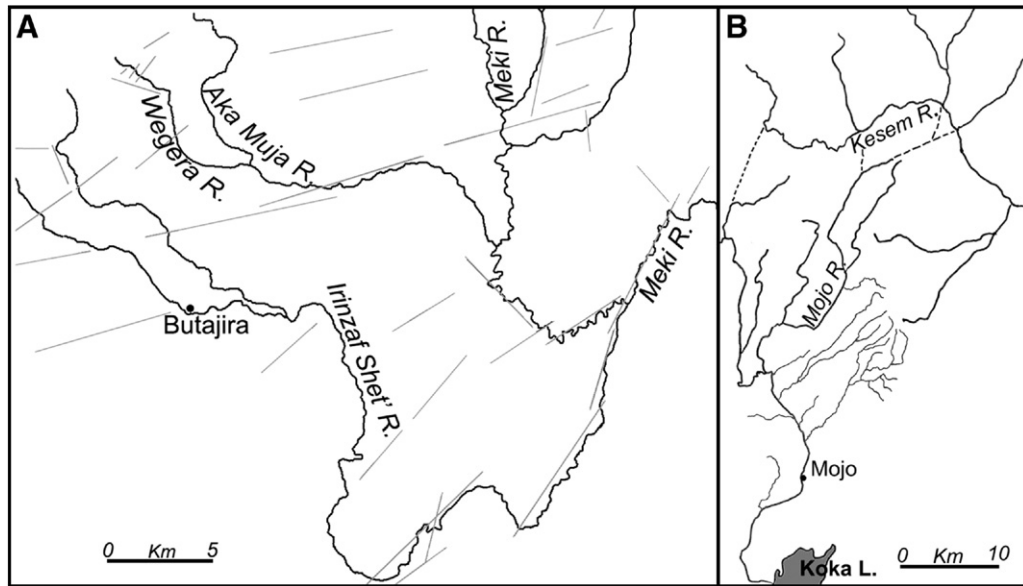
Fig. 5. (A) the Irinizaf Shet' in its upper reach NW of Butajira, as well as the Aka Muja river and Wegera river, tributaries of the Meki, flow along the local south-easterly slope as far as they abruptly turn to the northeast where they become controlled by the Silti–Debre Zeyt Fracture Zone System where they have been captured by the lower Meki river (redrawn from 1:250,000 Topographic Map of Ethiopia, Nazret Sheet, and from Bekele et al., 1992); (B) the Mojo river captured in its upper reach by the Kesam river flowing to the Afar depression (redrawn from 1:500,000 Tactical Pilotage Chart, Sheet TPC K-5C, 1982).

the Irinizaf Shet' in its upper reach NW of Butajira, as well as the Aka Muja river and Wegera river, tributaries of the Meki, flow along the local south-westerly slope as far as they abruptly turn to the northeast where the lower reach of the Meki become controlled by the Silti–Debre Zeyt Fracture Zone System (Fig. 5A).

The Awash and Mojo, the major rivers of the northern MER, show a distinctive pattern as well: 1) on entering the Rift, the Awash runs approximately southward. At Ombole it turns sharply eastward and maintains this direction as far as Koka reservoir (Fig. 3A and G). Before the dam construction the Awash river flowed to NE following the Wonji Fault Belt (East Africa 1:500,000 Topographic Map, Addis Ababa Sheet, 1946). Beyond the Koka dam, the Awash cuts across the Wonji Fault Belt and proceeds to the east, toward the Afar depression. This latter river reach is characterised by alternating deep gorges and swampy areas associated with fairly active horst and graben structures; 2) the Mojo river system follows the southward-trending regional slope developing a trellis, sub-parallel pattern, under the influence of volcanic and tectonic structures (Fig. 5B) and then turns east at right angle near Koka reservoir, which masks the former confluence with the Awash (see 1:500,000 East Africa Topographic Map, 1946). Moreover, the upper reaches

of the Mojo were captured by the Kesem river, which flows to the Afar depression (Fig. 5B), suggesting the past catchment of the Mojo was larger than the modern one.

3.2. Morphologic and geologic features

Gentle depressions stretch in a NNE–SSW direction, across the divide between Awash and Meki rivers (Fig. 6). They are presently occupied by either misfit ephemeral streams (their flow and channel morphology are clearly undersized with respect to the valley size) or ephemeral pools and marshes. Some of the ephemeral streams have reversed their flow direction, even in the last decade, as the local gradient is not yet well established because of the recent uplift of structural thresholds (such as the one between the Minko and the Sulula Hafa river-systems).

Three of the largest and continuous depressions, Koye, Fesesa and Cheleleka–Sulula Hafa, are aligned with the Awash upstream of Ombole village and with the Mojo upstream of the Gora Marsh, respectively (Fig. 6). The Cheleleka valley has an incised, meandering shape (Figs. 6 and 7), and a semi-permanent lake occupies its bottom.

The size of the Meki river valley, the Cheleleka paleovalley, the drowned paleovalley on the bottom of

Fig. 6. Satellite image of the study area. The prominent geomorphologic features are the NNE trending paleovalleys (Fesesa, Koye and Sulula-Hafa) lined up with the upstream reaches of the Awash and Mojo rivers.

Ziway lake (Aermap, 1969) and that of the upper reach of the Bulbula river are similar (Fig. 8). This suggests that a river, larger than the modern Meki and Bulbula rivers, flowed southward inside these valley reaches (see Section 5).

The Meki and Ketar rivers built up composite deltas in the northern sector of Ziway Lake (Figs. 1 and 6). The Meki river catchment covers approximately 2433 km^2 and bankfull discharge is about 70 m^3 s^{-1} (Ethiopian Ministry of Water Resources, unpublished data). The Ketar River catchment is 3350 km^2 with a bankfull discharge of 78 m^3 s^{-1} (see Table 2). In spite of the smaller catchment size, the Meki river delta is over ten

times larger than that of the Ketar, even after taking into account the submerged portions (Fig. 8). As the two basins do not differ significantly in their main characteristics (morphology, local relief, and lithology), the larger delta was probably formed by a larger paleoriver (see Section 5).

The eastward tilting of the Rift floor influenced the drainage network in the area. According to Abebe et al. (2005), the top of the Pleistocene fluvio–lacustrine deposits stands at an elevation of 1750 m asl in the Ombole area, on the western margin of the rift, whereas on the eastern side, in the area of Gore Marsh and Koka reservoir, it is found at 1600 m asl.

Another significant structural feature is the occurrence of gentle rolling ridges (small thresholds of Sagri, 1998), such as the Dubeta threshold (Fig. 2 C), expression of open anticlines deforming the fluvio–lacustrine and volcanoclastic deposits of up to Late Pleistocene age. In particular, the limbs of the WNW-ESE trending anticline coinciding with the Dubeta threshold dip 8°–10° NNE and SSW. This structure can be traced from the Fesesa palaeovalley to the west to the foots of the Bora volcano to the east. It forms a flat ridge 20 km long and 10 km wide with a maximum height of about 1700 m asl and an elevation of 40 m above the Meki River.

3.3. Stratigraphy and sedimentology

Further evidence of significant changes in river network during the Late Quaternary was found in several stratigraphic sections of Upper Pleistocene deposits, measured in the Meki river valley.

3.3.1. Meki River sedimentary logs

Three logs were obtained from up to 40 m high escarpments of the Meki river valley, cutting through the top of Pleistocene succession. These exposures are located a few kilometres upstream of the Meki–Cheleleka confluence, lined up with the Koye and Fesesa misfit valleys (Fig. 6). The exposed sedimentary succession is similar to that outcropping in the plain between Ziway and Abijata–Langano lakes and developed during the Late Pleistocene Megalake and Reduced Lake phases (Benvenuti et al., 2002, 2005).

With reference to the detailed stratigraphy described by Benvenuti et al. (2005) east of Lake Ziway (Gademota area, Fig. 2B) the succession in the Meki valley consists of the following six units (Fig. 9):

1) Fluvio–lacustrine sands and mud, up to 5 m thick (Fig. 9, log 3); medium-to coarse-grained sand and, subordinately, rippled or planar laminated silt.
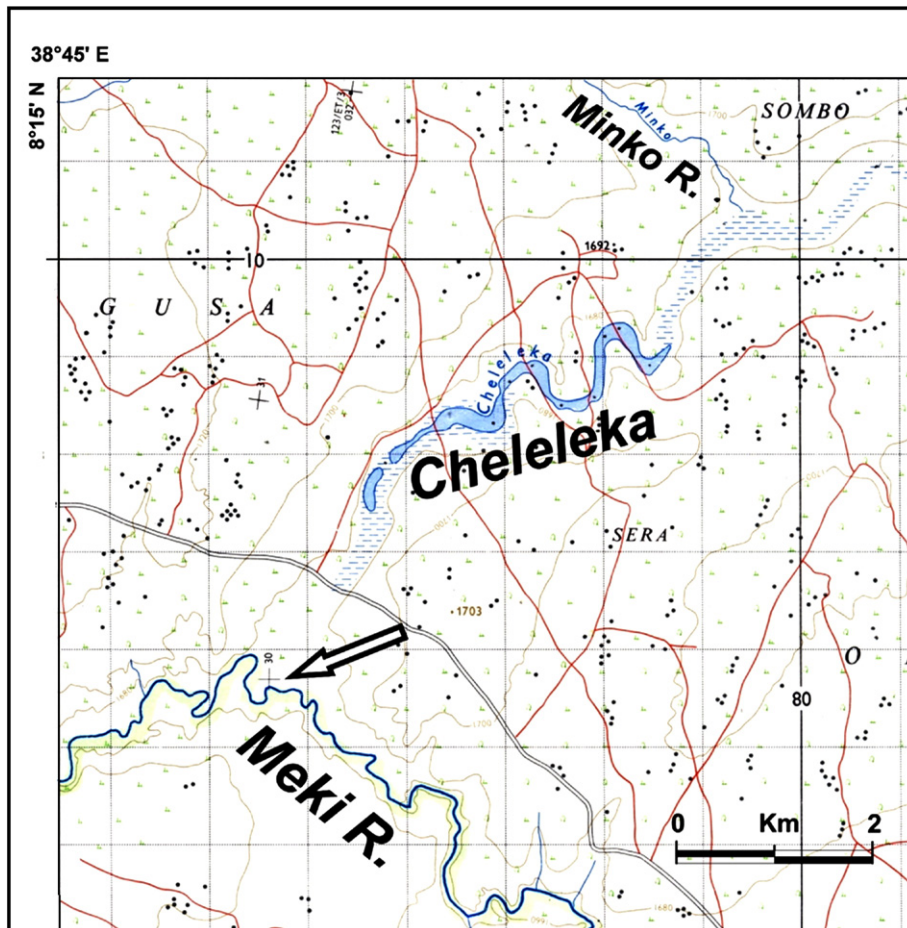

Fig. 7. The Cheleleka meandering valley and its ephemeral lake. The arrow indicates the cross-section exposed at the confluence with the Meki river (after the 1:50,000 topographic map of Ethiopia, Meki Sheet).
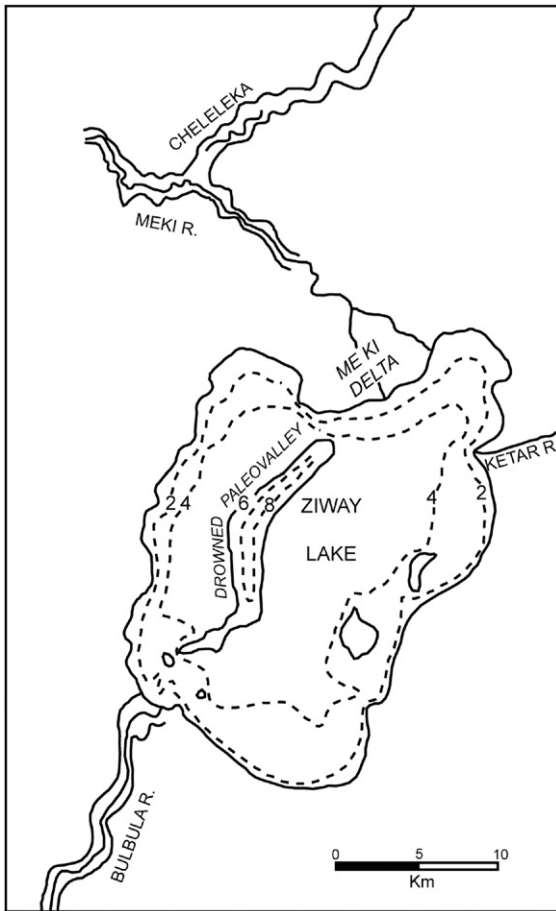
Fig. 8. Similarity in shape and width of the Cheleleka paleovalley, the paleovalley presently drowned in the Ziway Lake bottom and the Meki and Bulbula rivers valleys. Depth contours in meters (redrawn from 1:50,000 topographic map of Ethiopia–Meki and Ziway Sheets and Aermap, 1969).

Composition is mainly volcanogenic with abundant rounded pumice clasts.

2) Alluvial sands and mud, up to 3 m thick (Fig. 9, log 3); massive, medium-to fine-grained sand and silt, characterized by diffuse root bioturbation. This unit records a flood plain environment, marking a significant lake regression.

3) Subaerial volcanoclastic deposits, up to 14 m thick (Fig. 9, logs 1 and 3); sand-and silt-sized ashfall deposits, with dispersed pumice clasts, generally massive and subordinately planar laminated, with abundant root traces.

4) Above a high-relief erosion surface, fluvial gravels, sands and mud outcrop (Fig. 10A and B).

In log 1 this unit consists of gravels, and subordinately sands, up to 4 m thick. Pebbles are made of

basalt, or subordinately by ignimbrite and tuff, well rounded and clast-supported with interstitial sandy matrix. Gravels are arranged in decimetre-to meter-thick planar and trough cross-beds, indicating a palaeocurrent from the NW. Gravels are abruptly overlain by up to 3 m of yellowish sandy silt, in decimetre-to metre-thick crude horizontal beds, representing flood-plain deposits.

In log 2, the gravel beds are about 4 m thick and consist of clast-supported, well-rounded pebbles and subordinately cobbles. These deposits are arranged in amalgamated planar and trough cross-beds indicating a palaeocurrent from the NE. The gravels are overlain by pebbly sands and massive mud, bearing root traces, and capped by a poorly developed buried soil.

The top of log 3 is represented by gravels up to 1.80 m thick and truncated by terraced deposits of the Meki river. Gravels are similar in texture and composition to those observed in logs 1 and 2, with trough cross-beds indicating a palaeocurrent from the WNW.

On the whole, unit 4 shows typical features recording the development of a braided-river alluvial plain. Disseminated vertebrate remains in the deposits were unsuitable for radiocarbon dating.

5) Reworked pumice and tuff, up to 8 m thick, resting erosively on unit 4; coarse-to medium-grained volcanoclastic sand with abundant, well-rounded, pumice clasts. Subordinately, lithic clasts occur, mostly rhyolite and basalt, ranging from fine pebbles to granules. These sediments are interpreted as being deposited in a fluvio–lacustrine setting.

6) Yellowish sandy silt, bearing isolated lithic clasts, arranged in internally massive, decimetre-thick, horizontal beds. Textural features indicate *en masse* transport and deposition from subaerial debris flows. Large carbonate concretions on top belong to the petrocalcic horizon of the T'ra geosol, which covers all the surrounding flat surface, level with the Megalake lacustrine terrace (Carnicelli et al., 2002; Benvenuti et al., 2002).

Organic materials suitable for radiometric dating have not been found in the deposits of the Meki sections. Nevertheless, a physical correlation, based on lithological and facies similarity, is attempted with stratigraphic units established on the northern flanks of the Gademota Ridge, about 25 km south the study area (Table 1) (Benvenuti et al., 2002, 2005; Carnicelli et al., 2002, 2005). Despite their relative distance, both sites are located at the western margin of the Megalake system (Fig. 2B), making the facies development comparable. The facies stacking pattern at the two sites outlines a

similar transition of depositional environments (Table 1) evolving from marginal lacustrine (units 1 and 1c respectively) to volcano-alluvial (units 2, 3, 4 and 2a, 2b respectively), to fluvio–lacustrine (units 5 and 2c, respectively) and finally to slope settings (units 6 and 2d, respectively).
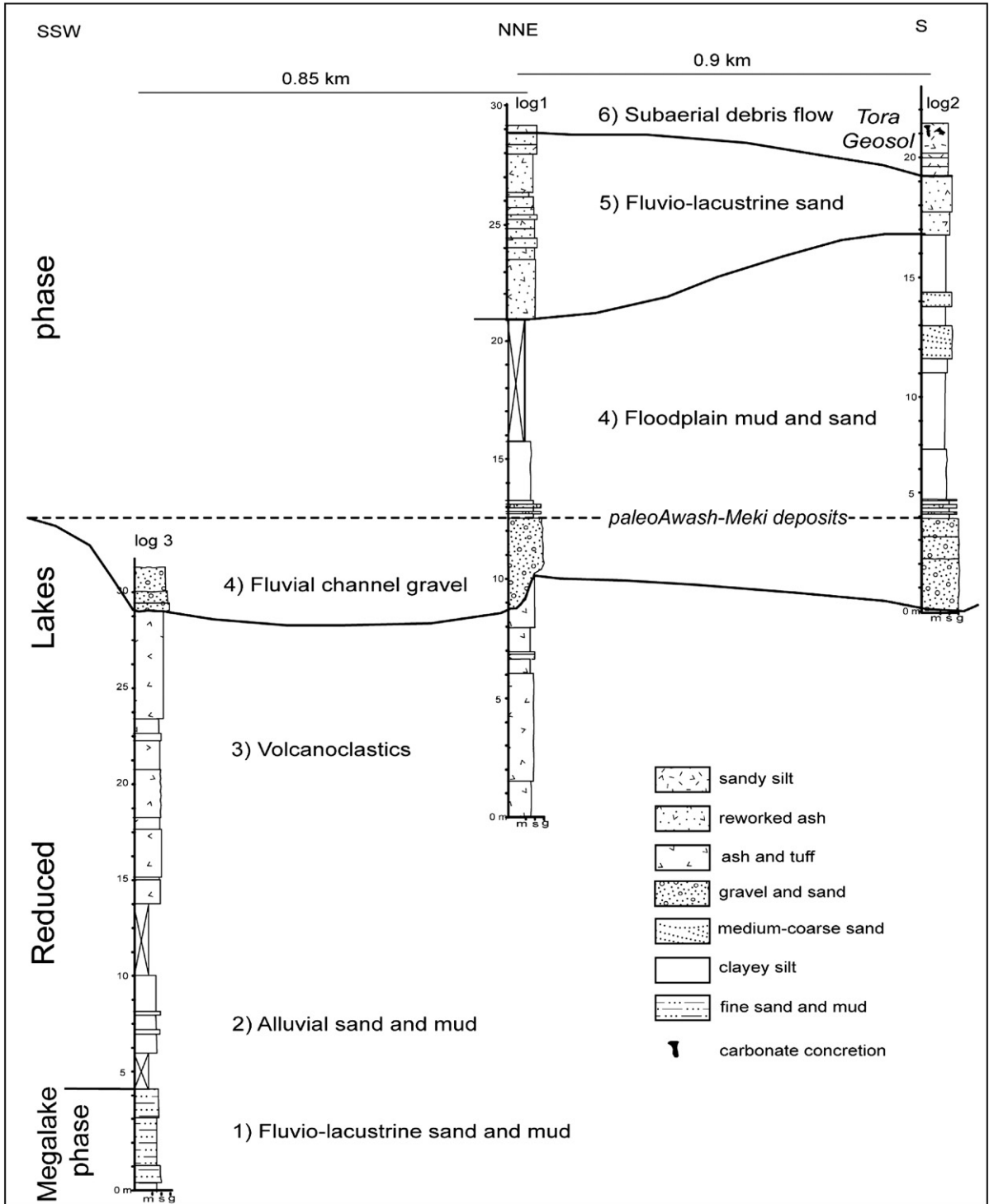

Fig. 9. Stratigraphic logs of the Upper Pleistocene deposits in the Meki river valley. (For location, see Fig. 6.)
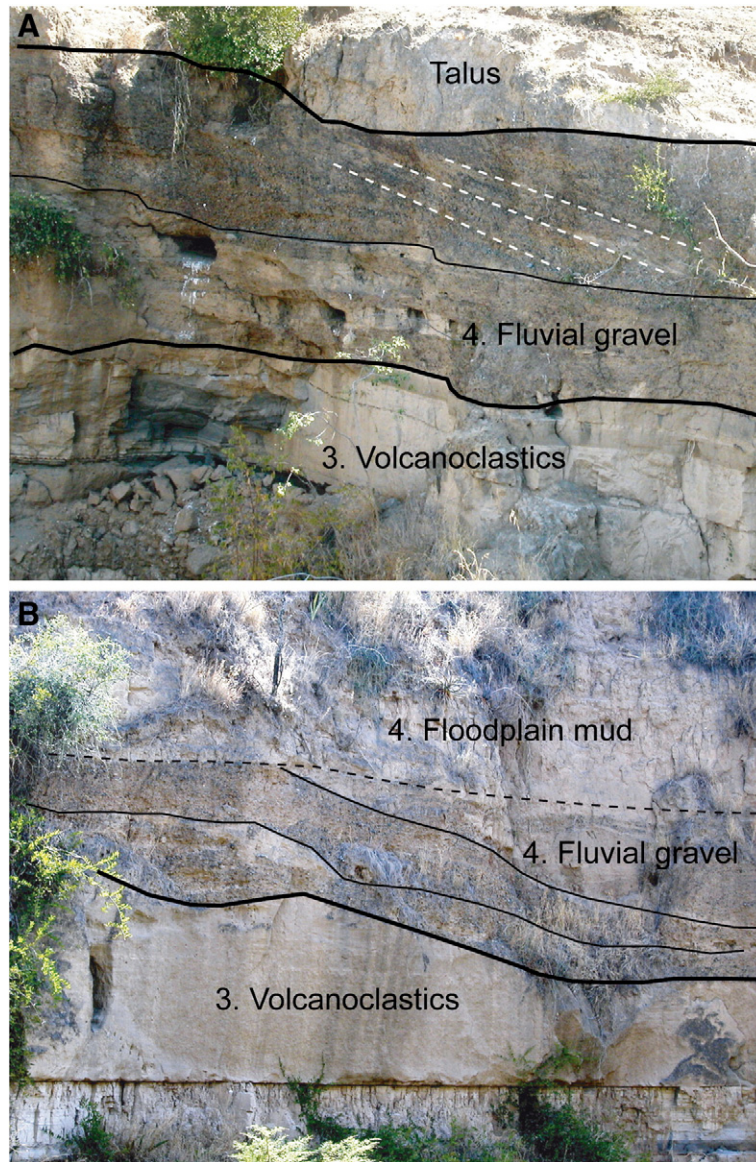
Fig. 10. A) Outcrop of the paleoAwash river gravel between log 1 and log 2 sites. Notice the planar cross stratification in the upper portion outlining a channel bar. The outcrop is about 5 m high; B) paleoAwash river channelized gravels and sands at log 1 site overlain by floodplain mud. The outcrop is about 5 m high.

3.3.2. Meki–Cheleleka confluence sedimentary logs

A good exposure was located at the confluence of the Cheleleka and the Meki river (Fig. 7), along the left bank of the latter and transverse to the dry valley. The succession is 4 m thick, displaying the sediment fill of the Cheleleka valley, and can be subdivided into two units (Fig. 11):

1) One meter thick layer of pebbles arranged in decimetre-thick horizontal beds separated by 1–2 cm of massive, coarse-grained sand. Pebbles are well rounded, clast-supported with a sandy matrix, and are made up mainly of basalt, with subordinate ignimbrite and tuff.

The largest clasts intermediate axis ranges from 3 to 5 cm and particle imbrication indicates a paleocurrents from the NNE.

2) Silty sand layer, 3 m thick, arranged in 10–15 cm planar cross beds, dipping 8°–10° (Fig. 11). Sands are massive or trough cross-laminated, indicating paleocurrents from the NE. Small pebbles are either scattered within the sand, or concentrated at the base of the trough cross-laminae. Convolute laminations occur at the base.

The stratification arrangement and facies association, showing epsilon cross-bedded sand, coarse grained channel lag, and horizontal overbank fine-grained

Table 1
Stratigraphic correlation of the Upper Pleistocene successions cropping out on the Meki River banks (this study) and on the Gademota area (from Benvenuti et al., 2002, 2005)

Meki River banks	Gademota area	Depositional phases
T'ora Geosol	T'ora Geosol (10–5 ky)	Macrolake
6) Subaerial debris flow	Alluvial and colluvial gravel, sand and mud (sub-unit 2d)	
5) Fluvio–lacustrine sand (reworked pumice and tuff)	Deltaic sand (reworked pumice and tuff, sub-unit 2c)	Reduced lakes
4) Fluvial gravel, sand and mud	Subaerial tuff and alluvial mud (sub-unit 2b, post-19 ky)	
3) Subaerial volcanoclastic deposits		
2) Alluvial sand and mud	Alluvial gravel and sand (sub-unit 2a,)	
1) Fluvio–lacustrine sand and mud	Fluvio-deltaic and lacustrine sand and mud (sub-unit 1c, 22 ky)	Megalake

topsets (Fig. 11) are typical of a meandering river. Its channel was oriented similar to the modern Cheleleka valley and the clast imbrication within the channel lag indicates flow from NNE towards the Meki river.

Only a thin veneer of alluvial and colluvial deposits caps the Cheleleka valley succession. The fluvio–lacustrine and subaerial sediments of units 5 and 6 of

Meki sedimentary logs (Fig. 9) are absent, as is the T'ora Geosol. This suggests that the final abandonment of the Cheleleka valley took place later than that of the Koye and Fesesa valleys.

Common to all river-channel sediments observed in the measured sections is the dominance of well-rounded basalt pebbles that, according to regional geology, should have been transported from the relatively distant north-western Rift margins.

3.4. Paleohydrology

The existing reconstructions of past hydrography and hydrology (Venzo, 1971; Street, 1979; Benvenuti et al., 2002) imply different interpretations of the evolution of the lake system (Street, 1979; Gillespie et al., 1983; Le Turdu et al., 1999; Benvenuti et al. 2002). To check the hypothesis that a large river flowed through the Cheleleka into the Meki river the hydrology of the modern rivers within the study area was investigated and a paleohydrologic reconstruction was attempted.

Wolman and Miller (1960) define the "dominant discharge" as the flow that performs most work in terms of sediment transport and, in the long term, yields the largest part of the sediment load. Many authors (Wolman and Leopold, 1957; Leopold et al., 1964; Ackers and Charlton, 1970) associate bankfull flow with dominant discharge and give it a relevant geomorphologic
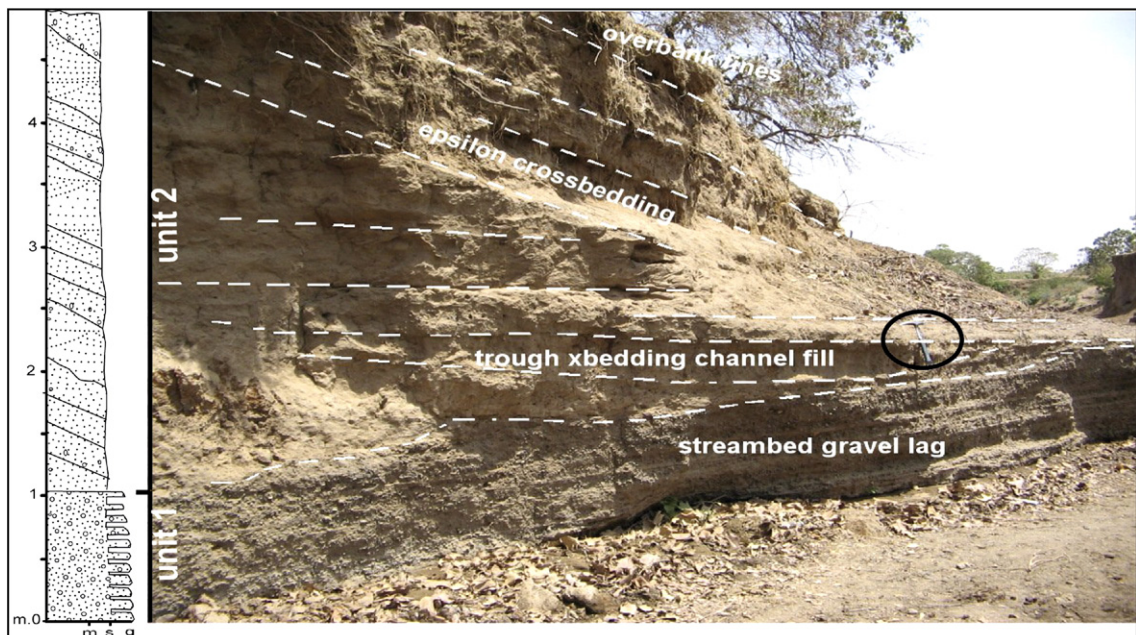

Fig. 11. Stratigraphic log and fluvial deposits filling the Cheleleka paleovalley at the confluence with the Meki river.

Table 2
Bankfull discharge (Q_b) [m³/s] of the study area rivers

River	Area (km²)	Lognormal		Gumbel EV1		Mean Q_b
		$Q_{1.58}$	$Q_{2.33}$	$Q_{1.58}$	$Q_{2.33}$	
Meki at Meki town	2433	61	75	65	79	70
Mojo at Mojo	1264	81	113	89	121	101
Awash at Ombole	7656	336	370	340	377	356
Ketar at Abura	3350	65	86	69	91	78

significance, since channel parameters such as hydraulic geometry or meander wavelength are adjusted to it. For these reasons, bankfull discharge can be considered as the most appropriate discharge when comparing channel pattern, morphology, flow hydrology, and sediment yield of different river systems.

There is some uncertainty among the authors about which discharge best approximates bankfull discharge. From field evidence, however, most of them (Leopold et al., 1964; Andrews, 1980; Torrizzo and Pitlick, 2004) restrict bankfull flow to a discharge with a return interval ranging from 1.58 to 2.33 years. Table 2 reports the bankfull flow data with 1.58 and 2.33 years return time calculated by both a lognormal interpolation and the Gumbel EV1 method, using daily flow data and spanning three decades. The mean values in Table 2 are the arithmetic means of all the data and are reported as a reference, to ease the comparison among modern river flow data and palaeo-bankfull discharge of Cheleleka, obtained by different methods (Table 3).

The paleochannel geometry data of Cheleleka (Fig. 7), the grain size of the channel lag deposits exposed near the confluence with the Meki river (Fig. 11), and the bed gradient were used to estimate flow velocity by the Chezy equation. Bed gradient was assumed to be the same as the present general slope of the valley floor, which is of the same order of magnitude of that present-day Meki river (0.001). The Darcy–Weisbach roughness coefficient was calculated by the Limerinos equation (Limerinos, 1970), which may be more appropriate than others given the gravelly bed. The flow velocity derived in this way was then introduced in the continuity equation to obtain bankfull discharge (Table 3). Several empirical models were also used for the same purpose. The results, listed in Table 3, show a relatively wide range (145–685 m³ s⁻¹); even the lowest values, however, are higher than the bankfull discharge of the modern Meki (70 m³ s⁻¹). The arithmetic average of all results is 313 m³ s⁻¹; that is, very close to the bankfull discharge of the modern Awash at Ombole (Table 3).

The wavelength of the Cheleleka meanders is 900 m (Fig. 7), whereas that of the modern Awash river near the confluence with the Sulula Hafa averages 800 m. This is another strong similarity between the Cheleleka and the Awash. Moreover, if the meander wavelength of the Cheleleka is reckoned by using the equations of Leopold and Wolman (1960) and Schumm (1972), based on bed gradient, bankfull width, and maximum depth, at the channel cross-section exposed at the confluence with the Meki , values of 676 and 677 m, respectively, result.

The available data (Table 3) indicate that the bankfull discharge of the river that flowed in the Cheleleka palaeovalley, south-west towards the present Meki, was in the range of 190–400 m³ s⁻¹ (12 results out of 17). Seven of the 17 models used predict a bankfull discharge higher than that of the modern Awash (356 m³ s⁻¹). To account for this result, either contribution from another river, or significant differences in rainfall pattern, and/or runoff coefficient of the watershed need considering. At near-present conditions, contribution from the Mojo is a good possibility.

Table 3
Bankfull discharge (Q_b) [m³/s] of Cheleleka R. calculated by different methods and equations

Author	Q_b	Parameters	Comments
Field data (this study)	199	A_b, D_{84}, J, R	Uniform flow; Chezy + Limerinos (1970)
Iglis (1948)	282	L_w	
Iglis (1948)	383	L_w	Incised meanders
Carlston (1965)	390	L_w	
Dury (1976)	292	L_w	
Dury (1977)	400	L_w	
Ackers and Charlton (1970)	296	L_w	
Ferguson (1975)	166	L_w	$Q_{1\%}$
Williams (1984)	390	L_w	
Leopold and Wolman (1957)	283	J	
Cheetham (1980)	627	J	
Henderson (1961)	685	J, D_{50}	
Williams (1978)	128	J, A_b	
Rotnicki (1991)	205	J, A_b, h	
Rundquist (1975)	391	J, h, S	
Charlton et al. (1978)	194	J, W_b	British gravel-bed rivers
Osterkamp and Hedman (1982)	171	W_b	Missouri rivers
Schumm (1972)	145	W_b, h_{max}	
Mean	313		
Standard deviation	156		

L_w = meander wave length; J = gradient; S = sinuosity; A_b = bankfull cross-section area; R = hydraulic radius; h = mean bankfull depth; h_{max} = maximum bankfull depth; W_b = bankfull width; D_{84} and D_{50} = particle diameter by which the 84 and 50%, respectively, of the sediment is finer; $Q_{1\%}$ = discharge [m³/s] equalled or exceeded 1% of the time.

4. Discussion

The Fesesa, Koye and Cheleleka paleovalleys, stretching in a north-south direction across the divide (Dubeta col) between the Awash and the Meki (Fig. 6), and their deposits indicate the existence of an ancient drainage network and allow the reconstruction of its evolution in space and time.

Venzo (1971) interpreted the Cheleleka paleovalley as being cut by the Meki, flowing north to join the Awash. Street (1979) considered the valley to have acted as the outlet of a Holocene lake (Macrolake of Benvenuti et al., 2002). The shape of Cheleleka valley, the paleohydrological analysis, the occurrence of fluvial gravels (see Section 3.3.2) indicating a southward paleocurrent, and the connections with the Meki to the south and the Awash to the north suggest instead that this valley was formed by a southward flowing river much larger than the present-day, ephemeral Sulula Hafa, and even larger than the Meki. Furthermore, the similarity in shape and width of the Meki valley, of the Cheleleka paleovalley, of the drowned paleovalley on the bottom of Ziway lake and that of the upper reach of the Bulbula river (Fig. 8), indicate that a river, larger than the modern Meki and Bulbula rivers, flowed southward inside these valley reaches.

The Fesesa and Koye palaeovalleys were reshaped by slope processes and partially filled, suggesting an early abandonment by the trunk rivers. By contrast, the Cheleleka paleovalley bears the fresh marks of a large meandering river (Fig. 7) which abandoned its valley later than the other two.

Evidence suggests that, initially, the Awash flowed south within the Fesesa and Koye paleovalleys; after receiving the Meki river, it turned southeast, along the present-day valley of the Meki (Fig. 12A). Also the Mojo flowed south through the area of the Gora Marsh, and proceeded through the Sulula Hafa–Cheleleka palaeovalleys to join the Awash–Meki river system, downstream of their confluence (Fig. 12A). The combined Awash–Mojo–Meki river system was of notable size, with a catchment about five times larger than that of the present day Meki river. This is witnessed by the fluvial gravels of the paleovalleys fill consisting of well-rounded basalt pebbles transported from distant sources on the high plains, beyond the northern margin of the Rift.

Later, the Awash river abruptly abandoned the Fesesa and Koye paleovalleys, swung to the East (flowing in a short reach of its modern valley) and joined the Mojo river, flowing through the Cheleleka palaeovalley (Fig. 12B). The Awash/Mojo river system, flowing into
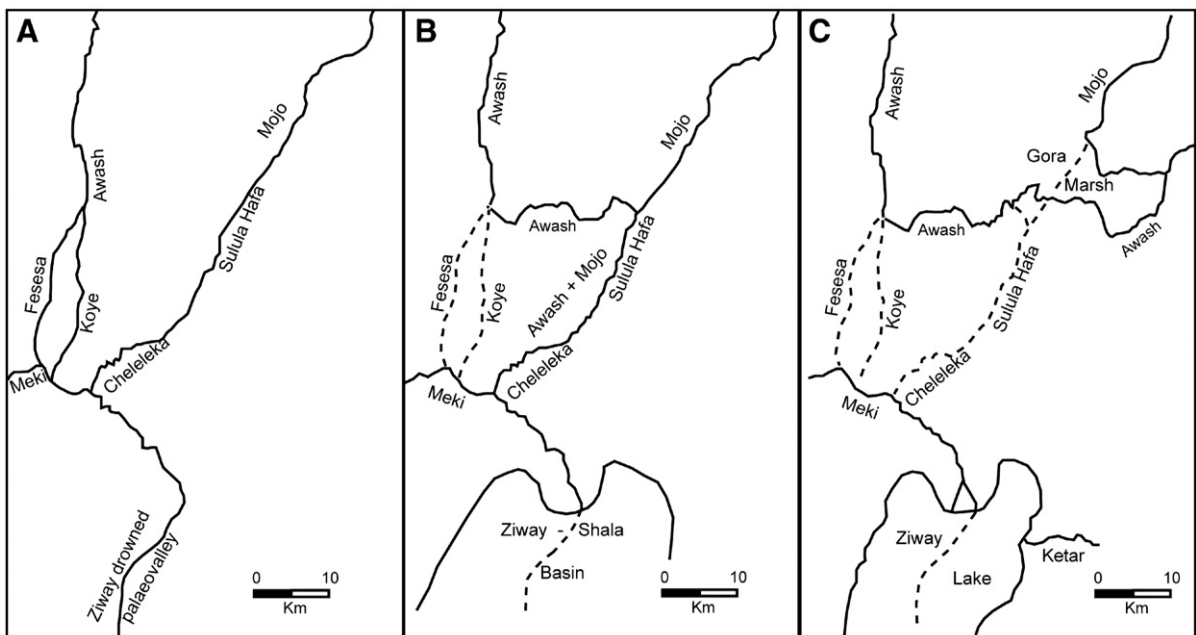

Fig. 12. Evolutionary stages of the main river network in the northern portion of the MER. (A) Pattern of the northern tributaries of the Pleistocene Megalake at the time of its shrinking (terminal Late Pleistocene); (B) the Awash abandonment of the Fesesa and Koye paleovalleys and its merging with Mojo into Cheleleka; (C) present-day river network after the eastward shift of the Awash and Mojo rivers. (Dotted lines indicate abandoned valleys.)

the Ziway–Shala lacustrine basin, widened the valley and formed broader meanders. Shortly later, the Awash river accomplished its eastward avulsion, abandoned the Cheleleka palaeovalley and took its present-day course, across the Wonji Fault Belt (Fig. 12C).

Despite the lack of precise chronologic calibration of the studied sections, the timing of the drainage network modification can be inferred with reference to the long-established Late Quaternary stratigraphic framework of the Lakes Region. This framework is based on numerous measured sections, about a hundred radio-metric age determinations (Laury and Albritton, 1975; Street, 1979; Gillespie et al., 1983; Bonnefille et al., 1986; Le Turdu et al., 1999; Benvenuti et al., 2002, 2005) and detailed regional correlation and mapping of Late Quaternary deposits (Benvenuti et al., 2002). The major lacustrine phases are the Upper Pleistocene Megalake (100,000–22,000 years BP) and the early-mid Holocene Macrolake (10,000–5,000 years BP). Their sediments are separated by a prominent ero-sional surface and, locally, by relatively thin volcani-clastic, alluvial, colluvial and fluvio-deltaic deposits (Reduced Lakes phase) ranging in age from 22,000 to 10,000 years BP. This interval includes the LGM and the latest Pleistocene post-glacial, on the whole char-acterized by significant aridity, causing dramatic lake regression, and intense volcanic activity in the MER (Gasse and Street, 1978; Benvenuti et al., 2002). The Koye and Fesesa paleovalleys are incised, filled and covered within the Reduced Lakes phase succession. The south-flowing paleodrainage must have then developed in the latest Pleistocene, specifically after 22,000 years BP, the younger age available for Megalake phase deposits (Table 1; Benvenuti et al., 2002, 2005).

The Cheleleka valley is instead incised in the top surface of the Reduced lake phase sediments, on which the T'ora Geosol developed during the moist early Holocene (10–5 ky BP; Carnicelli et al., 2002, 2005), suggesting that the eastward diversion of the regional drainage was completed during early Holocene.

The river network reorganisation took place due to opening of the Afar depression and eastward tilting of the Rift valley floor. Several additional factors contrib-uted to shape the new network. The occurrence of faults and fractures, transverse to the main rifting, controlled the eastward diversions of the main rivers, as exempli-fied by the sharp turns in the course of the Awash river near Ombole (Fig. 3G). The development of open anticlines, transverse to the Rift (Fig. 2C), had an important effect in influencing the river pattern. Finally, Late Pleistocene explosive volcanic activity (Di Paola, 1972; Street, 1979; Bigazzi et al., 1993; Le Turdu et al., 1999; Benvenuti et al., 2002; Abebe et al., 2005), emplacing huge volumes of pyroclastic materials, choked the rivers with excess sediment load, facilitating diversions.

5. Conclusions

During the shrinking of the Late Pleistocene Mega-lake, induced by LGM arid conditions, the main northern tributaries (Awash and Mojo), initially followed the lake shore retreat and incised the fluvio–lacustrine deposits, forming the Fesesa and Koye paleovalleys to the west and the Cheleleka palaeovalley to the east. The Awash–Mojo–Meki river system also carved the presently submerged palaeovalley of the Ziway Lake and the upper part of the Bulbula river valley (Fig. 12A).

After that, a generalised south-eastern shift of the drainage network, induced by tectonic movements, set in, and the Awash river, at first, left the Fesesa and Koye valleys, and joined the Mojo river through the Cheleleka valley (Fig. 12 B). At the end of Pleistocene, moist conditions allowed the development of the meandering valleys of Cheleleka, the initial rise of the Macrolake level in the Ziway–Shala Basin and the aggradation, at its northern margin, of an early Meki river delta (Fig. 12B). This was built up by the sediment transported by the Awash–Mojo–Meki river system.

Not long after, the southeastern shift of the drainage network was achieved and the Awash and Mojo rivers abandoned the Ziway–Shala basin, flowing towards the Afar depression (Fig. 12C). The loss of the Awash and Mojo rivers supply made the Macrolake smaller than the Megalake and therefore more susceptible to climate variations, as the late Holocene oscillations indicate. The decreased water inflow to the Ziway–Shala basin, combined with increased aridity in the Rift, determined the splitting of the Macrolake into the modern four lakes.

Despite a residual uncertainty about the precise timing of the regional drainage evolution, the case presented here has general conceptual implications for the understanding of hydrological processes in such highly dynamic geomorphic settings as the MER. Here, a complex drainage network development resulted from the complex interactions of climate, tectonics and volcanism.

In the Main Ethiopian Rift, therefore, climatic changes cannot be inferred from lake-level variations alone, as such variations are influenced by changes in water supply, caused by tectonic-induced rearrange-ments of the drainage networks.

Acknowledgements

References

Abbate, E., Sagri, M., 1980. Volcanites of the Ethiopian and Somali plateaux and major tectonic lines. Geodynamic Evolution of the Afro-Arabic Rift System, Accad. Naz. Lincei, Roma, Atti Convegni vol. 47, pp. 219–227.

Abebe, T., Manetti, P., Bonini, M., Corti, G., Innocenti, F., Mazzarini, F., Pécksay, Z., 2005. Geological map (scale 1:200,000) of the northern Main Ethiopian Rift and its implications for the volcano-tectonic evolution of the rift. Geol. Soc. Am., Map and Chart Series, 20 pp.

Ackers, P., Charlton, F.G., 1970. Dimensional analysis of alluvial channels with special reference to meander length. J. Hydr. Res. 8, 297–316.

Acocella, V., Korme, T., 2002. Holocene extension direction along the Main Ethiopian Rift, East Africa. Terra Nova 14, 191–197.

Aermap, 1969. Meki River diversion scheme: topographic surveys. Imperial Ethiopian Government. Awash Valley Authority, Addis Ababa. 14 pp.

Alessio, M., Allegri, L., Belluomini, G., Benvenuti, M., Cerasoli, M., Improta, S., Manfra, L., Sagri, M., Ventra, D., 1996. Le oscillazioni tardo-quaternarie del Lago Shala (Rift Etiopico): Analisi dell'evoluzione ambientale dall'integrazione di evidenze morfologiche, sedimentarie e cronologiche. Il Quaternario 9, 387–392.

Andrews, E.D., 1980. Effective and bankfull discharges of streams in the Yampa river basin, Colorado and Wyoming. J. Hydr. 46, 311–330.

Bekele, A., Boccaletti, M., Dainelli, P., Getaneh, A., Tortorici, L., 1992. Fracture pattern of the Main Ethiopian Rift area. Scale 1:500,000. S.E.L.C.A, Firenze.

Benvenuti, M., Carnicelli, S., Belluomini, G., Dainelli, N., Di Grazia, S., Ferrari, G.A., Iasio, C., Sagri, M., Ventra, D., Balemwald, Atnatu, Seifu, Ke., 2002. The Ziway–Shala lake basin (main Ethiopian rift, Ethiopia): a revision of basin evolution with special reference to the Late Quaternary. J. Afr. Earth Sci. 35, 247–269.

Benvenuti, M., Carnicelli, S., Ferrari, G., Sagri, M., 2005. Depositional processes in latest Pleistocene and Holocene ephemeral streams of the Main Ethiopian Rift (Ethiopia). In: Blum, M.D., Marriott, S.B., Leclair, S.F. (Eds.), Fluvial Sedimentology VII, Spec. Publs int. Ass. Sediment., vol. 35, pp. 277–294.

Bigazzi, B., Bonadonna, F.P., Di Paola, G.M., Giuliani, A., 1993. K–Ar and fission tracks ages of the last volcano-tectonic phase in the Ethiopian Rift Valley (Tulu Moye area). In: Abbate, E., Sagri, M., Sassi, F.P. (Eds.), Geology and Mineral Resources of Somalia and Surrounding Regions. Ist. Agronom. Oltremare, Firenze, Relaz. Monograf, vol. 113, pp. 311–322.

Billi, P., 1998. Climate. In: Sagri, M. (Ed.), Land Resources Inventory, Environmental Changes Analysis and their Application to Agriculture in the Lakes Region (Ethiopia), Final Report, European Commission, DG XII, Bruxelles, pp. 16–18.

Boccaletti, M., Bonini, M., Mazzuoli, R., Abebe, B., Piccardi, L., Tortorici, L., 1998. Quaternary oblique extensional tectonics in Ethiopian Rift (Horn of Africa). Tectonophysics 287, 97–116.

Bonini, M., Souriot, T., Boccaletti, M., Brun, J.P., 1997. Successive orthogonal and oblique extension episodes in a rift zone: laboratory experiments with application to the Ethiopian Rift. Tectonics 16, 347–362.

Bonnefille, R., Robert, C., Delibrias, G., Elenga, C., Herbin, J.P., Lezine, A.M., Perinet, G., Tiercelin, J.J., 1993. Palaeoenvironment of Lake Abijata, Ethiopia, during the past 2000 years. In: Frostic, L.E., Renaut, R.W., Reid, I., Tiercelin, J.J. (Eds.), Sedimentation in the African Rifts, Geol. Soc. London Spec. Publ., vol. 25, pp. 253–265.

Bull, W.B., 1997. Discontinuous ephemeral streams. Geomorphology 19, 227–276.

Carlston, C.W., 1965. The relation of free meander geometry to stream discharge and its geomorphic implications. Am. J. Sci. 263, 864–885.

Carnicelli, S., Benvenuti, M., Bonaiuti, F., Iasio, C., Sagri, D., Mirabella, A., Sagri, M., Ferrari, G.A., Belluomini, G., Wolf, U., 2002. The T'ora geosol (?) (Main Ethiopian Rift, Ethiopia): problems in defining palaeosols. Il Quaternario 15, 105–110.

Carnicelli, S., Benvenuti, M., Ferrari, G.A., Sagri, M., Mirabella, A., Terribile, F., 2005. Definition and genesis of a reference Geosol for the Main Ethiopian Rift (MER). Geophys. Res. Abstr. 7 [1607-7962/gra/EGU05-A-03990].

Charlié, F., Gasse, F., 2002. Late Glacial-Holocene diatom record of water chemistry and lake level change from the tropical East African Rift Lake Abiyata (Ethiopia). Palaeogeogr. Palaeoclimatol. Palaeoecol. 187, 259–283.

Charlton, F.G., Brown, P.M., Benson, R.W., 1978. The hydraulic geometry of some gravel rivers in Britain. Hydraulic Res. Station, Report It. 180 pp.

Cheetham, G.H., 1980. Late Quaternary palaeohydrology: the Kenneth Valley case study. In: Jones, D.K.C. (Ed.), The Shaping of Southern England. Academic Press, London, pp. 203–223.

Chernet, T., 1982. Hydrogeology of the Lakes Region, Ethiopia. Ministry of Mines and Energy, Addis Ababa. 97 pp.

Chorowicz, J., Collet, B., Bonavia, F.F., Korme, T., 1994. Northwest to north-northwest extension direction in the Ethiopian Rift deduced from the orientation of extension structures and fault slip analysis. Geol. Soc. Am. Bull. 105, 1560–1570.

Coetzee, J.A., van Zinderen Bakker, E.M., 1989. Palaeoclimatology of East Africa during the last glacial maximum: a review of changing theories. In: Mahaney, W.C. (Ed.), Quaternary And Environmental Research On East African Mountains. Balkema, Rotterdam, pp. 189–198.

Di Paola, G.M., 1972. The Ethiopian Rift Valley (between 7° 00, and 8°40'lat. North). Bull. Volcanol. 36, 517–560.

Dury, G.H., 1976. Discharge prediction, present and former, from channel dimension. J. Hydr. 30, 219–245.

Dury, G.H., 1977. Underfit streams: retrospect, perspect and prospect. In: Gregory, K.J. (Ed.), River Channel Changes. Wiley, Chichester, pp. 281–293.

East Africa 1:500,000 Topographic Map, 1946. Addis Abeba (Addis Ababa) Sheet NC-37/5. War Office, Geographical Section, London.

Ebinger, C.J., Yemane, T., Woldegabriel, G., Aronson, J.L., Walter, R.C., 1993. Late Eocene-Recent volcanism and faulting in the southern Main Ethiopian Rift. J. Geol. Soc. Lond. 150, 99–108.

Ferguson, R.I., 1975. Meander irregularity and wavelength estimation. J. Hydr. 26, 315–333.

Gasse, F., 1977. Evolution of Lake Abhe (Ethiopia and TFAI), from 70,000 BP. Nature 265, 42–45.

Gasse, F., Fontes, J.C., 1988. Palaeoenvironments and palaeohydrology of a tropical closed lake (Lake Asal, Djibuti) since 10,000 yr BP. Palaeogeogr. Palaeoclimatol. Palaeoecol. 69, 10–67.

Gasse, F., Street, F.A., 1978. Late Quaternary lake-level fluctuations and environments of the Northern Rift Valley and Afar region (Ethiopia and Djibuti). Palaeogeogr. Palaeoclimatol. Palaeoecol. 24, 279–325.

Gasse, F., Van Campo, E., 1994. Abrupt post-glacial climate events in West Asia and North Africa monsoon domains. Earth Planet. Sci. Lett. 126, 435–456.

Gèze, F., 1975. New dates on ancient Galla Lake levels. Bull. Geophys. Obs. Addis Ababa 15, 119–124.

Gillespie, R., Street-Perrot, F., Switsur, R., 1983. Post-glacial arid episodes in Ethiopia have implications for climate prediction. Nature 306, 680–683.

Graf, W.L., 1988. Fluvial Processes in Dryland Rivers. Springer-Verlag, Berlin. 346 pp.

Grove, A.T., Street, F.A., Goudie, A.S., 1975. Former lake levels and climatic changes in the rift valley of Southern Ethiopia. Geogr. J. 141, 177–202.

Henderson, F.M., 1961. Stability Of Alluvial Channels. ASCE, J. Ydr. Div., vol. 87, pp. 109–138.

Iglis, C.C., 1948. The behaviour and control of rivers and canals. CWINRS, India Res. Publ. 13 pp.

Lamb, A.L., Leng, M., Lamb, H.F., Mohammed Umer, M., 2000. A 9,000-year oxygen and carbon isotope record of hydrologic change in a small Ethiopian crater lake. Holocene 10, 167–177.

Laury, R.L., Albritton, C.C., 1975. Geology of the Middle Stone Age archaeological sites in the Main Ethiopian Rift Valley. Geol. Soc. Am. Bull. 86, 999–1011.

Leopold, L.B., Wolman, M.G., 1957. River channel pattern: braided, meandering and straight. US Geol. Surv. Prof. Pap. p. 282B.

Leopold, L.B., Wolman, M.G., 1960. River meanders. Geol. Soc. Am. Bull. 71, 769–794.

Leopold, L.B., Wolman, M.G., Miller, J.P., 1964. Fluvial processes in geomorphology. Freeman, San Francisco. 522 pp.

Le Turdu, C., Tiercelin, J.J., Gibert, E., Travi, Y., Lezzar, K.E., Richert, J.P., Massault, M., Gasse, F., Bonnefille, R., Decobert, M., Gensous, B., Jeudy, V., Tamrat, E., Umer Mohammed Mohammed, Martens, K., Balemwald, Atnafu, Chernet, Tesfaye, Williamson, D., Taieb, M., 1999. The Ziway–Shala lake basin system, Main Ethiopian Rift: Influence of volcanism, tectonics, and climatic forcing on basin formation and sedimentation. Palaeogeogr. Palaeoclimatol. Palaeoecol. 150, 135–177.

Limerinos, J.T., 1970. Determination of the Manning coefficient from measured bed roughness in natural channels. U.S. Geol. Surv., Water Supply Pap. 1898-B. 47 pp.

Meigs, P., 1953. World distribution of arid and semi-arid homoclimates. Reviews of Research in Arid Zone Hydrology. UNESCO, Paris, pp. 203–209.

Merla, G., Abbate, E., Azzaroli, A., Bruni, P., Canuti, P., Fazzuoli, M., Sagri, M., Tacconi, P., 1979. A Geological map of Ethiopia and Somalia, and comment. C.N.R., Firenze. 89 pp.

Mohr, P.A., 1962. The Ethiopian Rift System. Bull. Geophysics Obs. Addis Ababa 5, 33–62.

Osterkamp, W.R., Hedman, E.R., 1982. Perennial Stream Flow Characteristics Related To Channel Geometry And Sediment in Missouri River basin. US Geol. Surv. Prof. Pap., vol. I214, pp. 1–37.

Rotnicki, A., 1991. Retrodiction of palaeodischarges of meandering and sinuous alluvial river and its palaeohydroclimatic implications. In: Starkel, L., Gregory, K.J., Thornes, J.B. (Eds.), Temperate Palaeohydrology. Wiley, Chichester, pp. 431–471.

Rundquist, L.A., 1975. A classification analysis of natural rivers. Ph. D. thesis, Colorado State University, Fort Collins, Colorado.

Sagri, M.(Ed.) and the staff of EU Project, 1998. Land resource inventory, environmental change analysis and their application to agriculture in the Lake Region (Ethiopia). Final Report, European Commission, DG XII, Bruxelles, 183 pp.

Schumm, S.A., 1972. Fluvial paleochannels. In: Rigby, J.K., Hamblin, W.K. (Eds.), Recognition of Ancient Sedimentary Environments. Soc. Econ. Paleontol. Min. Spec. Publ., vol. 16, pp. 98–107.

Street, F.A., 1979. Late Quaternary lakes in the Ziway–Shala Basin, Southern Ethiopia. Ph.D. Thesis, Univ. Cambridge, 457 pp.

Street, F.A., Grove, A.T., 1979. Global maps of lake level fluctuations since 30,000 years BP. Quat. Res. 12, 83–118.

Tactical Pilotage Chart, 1982. TPC K5C 1:500,000 Ethiopia. US Defence Mapping Agency, St. Louis, Missouri.

Tefera, Mengesha, Chernet, Tadiwos, Haro, Workineh, 1996. Geological Map of Ethiopia 1: 2,000,000. Geological Survey of Ethiopia, Addis Ababa.

Torrizzo, M., Pitlick, J., 2004. Magnitude-frequency of bed load transport in mountain streams in Colorado. J. Hydr. 290, 137–151.

Venzo, G.A., 1971. Geological significance of an abandoned ancient channel across the Galla Lakes–Awash River watershed in Ethiopia. Studi Trentini Sci. Nat. 48, 243–254.

Williams, G.P., 1978. Bankfull discharge of rivers. Water Res. 14, 1141–1154.

Williams, G.P., 1984. Paleohydrologic equations for rivers. In: Costa, J.E., Fleisher, P.J. (Eds.), Development and application in Geomorphology. Springer, Berlin, pp. 343–367.

Woldegabriel, G., Aronson, J., Walter, R.C., 1990. Geology, geochronology and rift basin development in the central sector of the Main Ethiopian Rift. Geol. Soc. Am. Bull. 102, 439–458.

Wolman, M.G., Leopold, L.B., 1957. River Flood Plains: Some Observations On Their Formation. USGS Prof. Paper, vol. 282C, pp. 87–109.

Wolman, M.G., Miller, J.P., 1960. Magnitude and frequency of forces in geomorphic processes. J. Geol. 68, 54–74.